Analysis and Optimization of Additively Manufactured Propellers for Heavy Lift Drones

Daniel Hurley[1], Madison Lott[2], Cody Johnson[3], and Dalton Singleton[4]
Mississippi State University, Mississippi State, MS 39762

With the advent of widespread applications of drone technology, there is an increasing need to improve the performance of heavy-lift cargo drones. Standard off-the-shelf propellers are typically designed for general recreational use and are often not optimized for the specific demands of carrying heavy payloads. This study establishes a method to design and manufacture high-efficiency propellers using accessible additive manufacturing technology. Using aerodynamic simulation software, 325 different airfoil shapes were analyzed to find the most efficient profile for heavy lift operations. The analysis identified NACA 3117, 4118, and 5213 as the top three optimal airfoil shapes. A custom 16" propeller generated blades on this shape and was manufactured using Fused Deposition Modeling (FDM) with materials including ABS and Carbon Fiber reinforced PETG. These prototypes were tested on a test stand at speeds up to 6000 RPM. Testing showed that the XROTOR-designed propellers had tripled the efficiency of the APC propeller. By comparing the thrust, efficiency, and structural stability of these printed blades against a standard commercial propeller, this project demonstrates a low-cost way to create high-performance custom drone propellers.

Nomenclature

C	=	chord
C_d	=	coefficient of drag
C_l	=	coefficient of lift
C_m	=	moment coefficient
$\mathrm{C_Q}$	=	coefficient of torque
C_T	=	coefficient of thrust
D	=	drag
J	=	advance ratio
L	=	lift
Q	=	torque
r	=	radius
$\mathrm{R_a}$	=	surface roughness
Re	=	Reynold's number
RPM	=	revolutions per minute
T	=	torque
α	=	angle of attack (blade section)
μm	=	micron (micrometer)

[1] Student, Mississippi State Aerospace Engineering Department, AIAA Student Member 1424805
[2] Student, Mississippi State Aerospace Engineering Department, AIAA Student Member 1930775
[3] Student, Mississippi State Aerospace Engineering Department , AIAA Student Member 1930696
[4] Student, Mississippi State Aerospace Engineering Department , AIAA Student Member, 1930698

I. Introduction

The evolution of Unmanned Aerial Vehicles (UAVs) has evolved rapidly from early military concepts into essential tools for commercial logistics, cinematography, infrastructure inspection, and emergency response. Drone usage in everyday life is likely to continue growing, especially as companies like Amazon advance drone-based package delivery systems and the urban air mobility sector expands. This also means the operational requirements for these aircraft are becoming increasingly strict, shifting the design focus toward maximizing payload capacity and endurance. While standard production propellers serve general recreational purposes, they are often not optimized for the specific lift requirements of cargo operations. Additive manufacturing, specifically FDM (Fused Deposition Modeling) printing, has experienced a similar jump in accessibility in recent years. This accessibility enables engineers and the everyday man alike to rapidly prototype a multitude of complex designs that were previously difficult to manufacture, such as rapid aerodynamic prototyping.

This study, conducted as a Senior Design project for the Mississippi State University Department of Aerospace Engineering, seeks to combine theoretical aerodynamic optimization with rapid prototyping. The objective is to develop a methodology to optimize propeller geometries tailored for high-lift applications, then conduct experimental tests to validate the findings. While the focus of this paper is specifically on altering airfoil geometries, the methodology developed can be applied to various data sets and design parameters in later work.

II. Methodology

A. Scope Definition

Propeller design is an involved field with considerable depth and complexity; Therefore, given the limited resources of a senior design project, the developed propeller optimization methodology will be applied within a constrained scope. This allows for the optimization methods to be proven as effective, while also laying the groundwork for future work. The parameters that were identified as critical to airfoil and propeller design include: airfoil selection, propeller diameter and pitch, number of airfoils used in the blade of the prop, number of blades on the propeller, optimization parameters, manufacturing capabilities, and material selection. This study will focus specifically on optimizing propeller geometry for efficiency (Eq. 1).

$$\boldsymbol{\eta} = \frac{(\boldsymbol{C_T} \cdot \boldsymbol{J})}{\boldsymbol{C_Q}} \qquad (1)$$

For this project, the first step taken in developing a new propeller geometry was airfoil selection. The National Advisory Committee for Aeronautics (NACA) 4-series airfoils were selected for their simplicity and easily accessible properties. The terminology for the 4-series airfoils can easily be broken down into three parts. The first digit is a description of maximum camber as a percentage of chord length. The second digit is the distance of the maximum camber from the leading edge (front) of the airfoil in tenths of the chord, and the last two digits indicate the maximum thickness of the airfoils as a percentage of chord length. An example of the 4-series notation is the NACA 2412, which indicates a maximum camber of 2%, a maximum camber location of 40% chord length from the leading edge, and a maximum thickness of 12%. Upon selection of an airfoil classification, the scope was narrowed down to airfoils commonly used in heavy lift cargo scenarios. It was identified that airfoils from the 2000 and 4000 groups are commonly used in current drone propeller applications, so to be exhaustive, groups 2000 through 6000 were included in the dataset.

To ensure the resulting geometries could be manufactured via FDM, constraints were placed on the airfoil dimensions. The maximum camber varied from 2% to 6%. Maximum thickness values were restricted to a range of 6% to 18%; airfoils thinner than 6% challenge FDM capabilities, while those thicker than 18% yield diminishing aerodynamic returns. This filtering process resulted in a final dataset of 325 airfoils.

BEMT is most accurate for 17" diameter propellers [1], so 16" was selected for the diameter due to its commercial availability and proximity to BEMT's optimal propeller diameter.

To determine propeller pitch, the team referenced Advanced Precision Composites (APC)'s performance data for 16" propellers at various pitches. For each propeller, efficiency was plotted as a function of velocity. The 16x16 propeller (16 pitch) had the highest efficiency ratio over the longest range of velocities.

To simplify the optimization process, the number of airfoils used simultaneously in the propeller design was restricted to a single airfoil. Although some propeller configurations employ a thicker airfoil near the hub and a thinner one toward the tip, such variation substantially increases the complexity of the analysis and optimization. Consequently, this approach is excluded from the present study. While there are many different parameters that can be selected for optimization, such as noise performance, flutter, fatigue, and boundary layer attachment, our study will focus specifically on increasing prop efficiency with a goal of a 25% gain.

B. XFOIL

For this study, XFOIL was selected as the computational software for airfoil analysis due to the software's simplicity and light computation methods. This allows for a large airfoil sample size and the ability to test a wide range of angles of attacks without the need for extensive computing resources and time spent running complex CFD simulations. The simplicity of XFOIL arises from its treatment of airfoil geometries as infinitely thin surfaces, enabling the software to efficiently provide aerodynamic parameters such as C_l, C_d, and C_m [2].

Before XFOIL can supply a full set of aerodynamic variables, there are multiple conditions that need to be considered. The main conditions are the number of iterations performed by the simulator, the airfoil's angle of attack, and whether viscosity effects should be considered; if so, the Reynolds number needs to be specified. For this study, 1000 iterations were chosen due to the large angle of attack range, helping the solver converge upon a correct answer. Additionally, viscous analysis with a Reynolds number of 160,000 was selected, as this was the average of the 151,810 - 170,218 Reynolds number range used by the control APC propeller at 5,000 RPM [3]. An RPM of 5,000 was chosen due to it being the average operating condition of a heavy lift cargo drone, which usually ranges from 4,000 to 6,000 RPM [4]. To ensure solver convergence and capture the full operating range, the α was swept from -6° to 18° in 1° increments.

Due to X-foil having a command prompt user interface, individually modifying, and initializing each simulation would be far too time consuming. For this reason, a batch file was created which ran the 325 airfoils, saving the resulting polar from each airfoil to a directory, then reopening to run the next airfoil in the series.

C. Airfoil Ranking

Once XFOIL aerodynamic data was gathered for each of the 325 airfoils, they were ranked based upon most favorable operating conditions. Due to the lower RPM, a high C_l of 0.7 was chosen as the target value for ranking. Using MATLAB, each airfoil was ranked based upon their lift to drag ratio at $C_l = 0.7$. These values were read into an Excel sheet, which gave the top 3 NACA airfoils as 4118, 5213, and 3117, respectively (Fig. 1) [8]. The best airfoils from this list were further analyzed in XFOIL with smoother sequencing, going from α of -6° to 18° in 0.1° increments to ensure smooth transitions and data collection, barring some near-stall values.

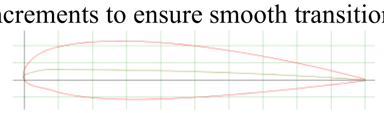

Fig. 1 (a) NACA 3117

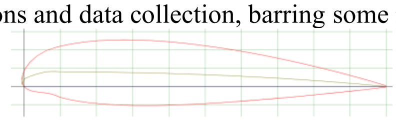

Fig. 1 (b) NACA 4118

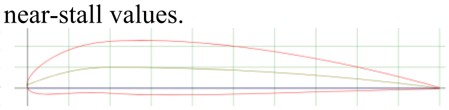

Fig. 1 (c) NACA 5213

D. XROTOR

Once the final aerodynamic data from XFOIL was supplied, the next step was to use computational software called XROTOR to create a full propeller geometry that satisfies a set of geometric and aerodynamic conditions. XROTOR relies on a similar command prompt style to XFOIL. However, unlike XFOIL, XROTOR uses a file that contains an aerodynamic polar to generate its data. As XFOIL's output gives individual aerodynamic data at each angle of attack respectively, rather than an entire aerodynamic polar, the data must be converted for proper aerodynamic analysis in XROTOR.

To perform the conversion between XFOIL aerodynamic data into an aerodynamic polar suited for XROTOR, a MATLAB script was developed which plots XFOIL's aerodynamic data, allowing for derivation of aerodynamic polar values, namely the change in C_l per change in α in radians, incremental change in C_l per change in α at stall, maximum and minimum C_l, change in C_l prior to stall, and more [8]. The change in C_l per change in α in radians was computed by finding the slope of the linear C_l /α curve, while the changes in C_l prior to and at stall were estimated to be 0.1. XROTOR's solver often approximates this value to be a low positive number to assist with the simulation process; in actuality, the change in lift coefficient at stall is negative.

Once the aerodynamic polar input was computed, a sanity check was performed by inputting the polar curve and retrieving the graph shown below in Figure 2. As the polar curve shows a consistent shockwave pattern (that being the leftmost graph with Mach number curvatures) and C_l/α curve (the rightmost graph illustrating change in C_l with respect to α), it can be assumed that the conversion performed from individual aerodynamic data to aerodynamic polar curvature is correct.

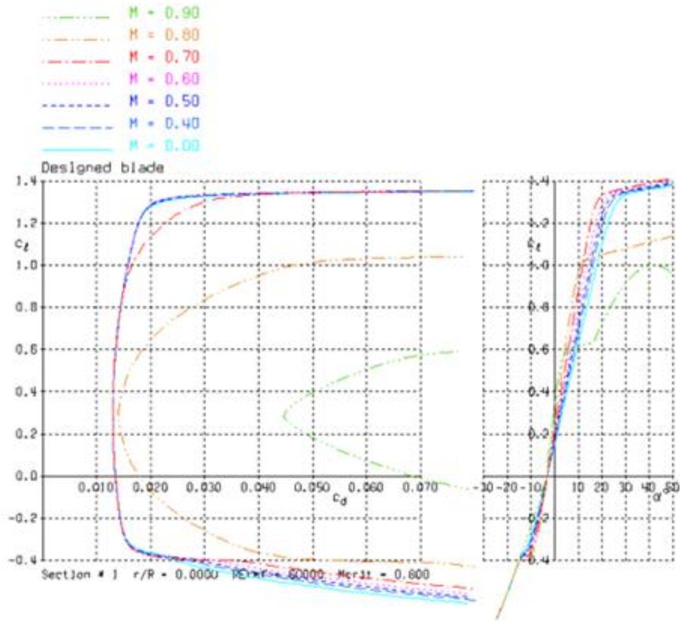

Fig. 2 XROTOR Aerodynamic PLOT

The last step in propeller generation using XROTOR was to input the geometric outline of the propeller, i.e., number of blades, width, and hub shape, as well as target values for lift coefficient, and the thrust at a certain RPM or power draw. Most of the design conditions are driven by APC propeller data at Re of ~160000. Two blades were chosen, along with an 8 " radius, 0.75 " hub radius, 0.779 " wake displacement radius, a relative airspeed of 57.85 mph, and a force of 16.676 N at 5000 RPM [3]. These geometric and performance values produced various propeller designs for each airfoil. The propeller produced for NACA 4118 is shown below in Figure 3.

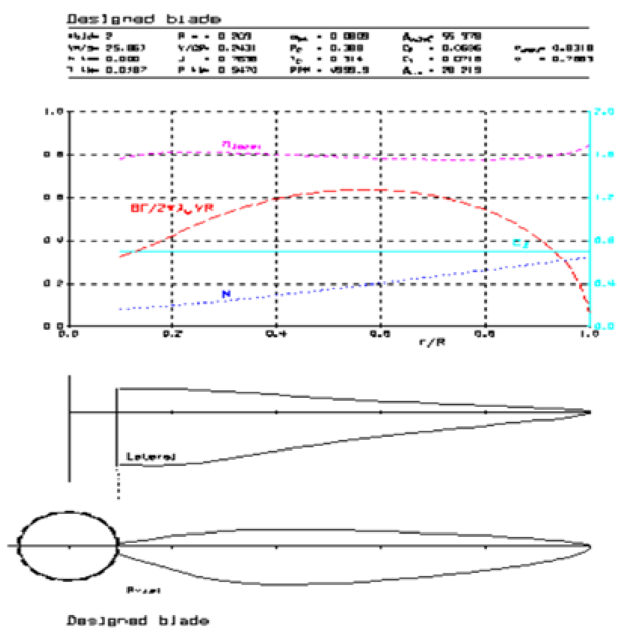

Fig. 3 XROTOR propellor design for airfoil NACA 4118

E. Additive Manufacturing & Materials Testing

Before our study began, a feasibility study was conducted to determine if printing a single 16” propeller on a Bambu Labs A1 printer was even possible. Using a 16x5.4 propeller from GrabCAD [5], a test print was sliced and printed. This proved that printing 16” propellers was within our capabilities.

Before printing the optimized propeller geometries, a filament material needed to be selected, and a smoothing method to reduce surface roughness needed to be established. APC’s 16x16 sport propeller [6] was chosen as a control for its surface roughness profile and shape. To ensure that significant differences in surface roughness do not impact the test results, the control propeller’s geometry was recreated using a Keyence VL-800 3D scanner. Due to the volumetric constraints of the Bambu A1 printer, the print orientations for a 16” propeller are limited. It was determined that rotating the blade 45 degrees about the z-axis, 35 degrees about the y-axis, and 83 degrees about the x-axis resulted in an orientation that fits on the build plate and reduces layer deformation. 100% infill was selected to provide maximum strength, and tree supports were auto generated with a threshold angle of 60 degrees (See Figure 4).

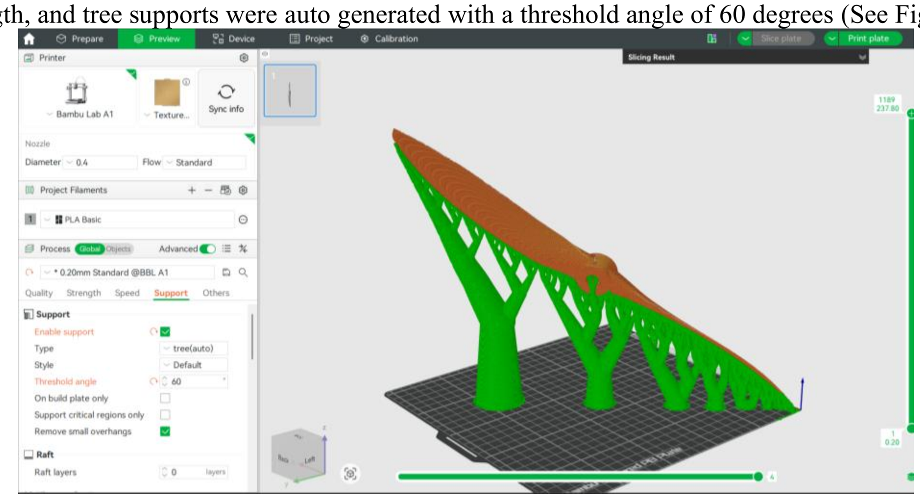

Fig. 4 APC 16x16 geometry in Bambu Studio sliced for printing

Material selection was conducted through survivability testing of four filament candidates: PLA, PETG, PETG-CF, and ABS. Each material was used to print the geometry of the control propeller and then subjected to structural testing on a rotor test stand, as it was suspected that at least one of the materials would suffer from catastrophic structural failure. Each propeller was operated at 6000 RPM, 1000 RPM above the RPM range of the perceived application for these propellers, to determine if the materials could withstand sustained operation, 2 minutes, at elevated rotational speeds without structural failure or deflection. High-speed video was taken during the operation of the test stand to assess blade deflection and potential flutter. From this round of testing, seeing no structural failure and marginal flutter differences between materials, it was determined that each material was strong enough, and additional testing would be needed to determine the ideal printing filament. A focus on replicating the surface finish of the APC propeller with the additively manufactured propellers was then taken. Because fused deposition modeling produces components through a layer-by-layer deposition process, surface irregularities such as layer lines and minor printing imperfections are to be expected. These imperfections increase drag and could reduce overall efficiency.

Therefore, four separate methods to decrease surface roughness were tested and evaluated. Two propellers of the scanned APC geometry were printed in each material option. From there, each blade of the test article propellers was finished and smoothed using a different technique: sanding alone, application of paint primer followed by sanding, sanding followed by application of a Bondo-acetone mixture, and application of the Bondo-acetone mixture before sanding. Using a Keyence VR machine, the surface roughness (R_a) of the control propeller, the untreated propellers created from each material, and each different finishing method on each material was measured and compared, as seen in Table 1 and Figures 5 and 6. The control propeller has a measured surface roughness of 3.704 μm . The material and method combination that produced a surface smoothness as close to the control propeller at 3.735 μm was ABS that was painted with acetone-thinned Bondo Glazing and Spot Putty and then sanded.

Table 1 Comparison of Propeller Surface Roughness in Microns

Propeller Type	Untreated	Sanding Only	Paint Primer + Sanding	Bondo-Acetone Before Sanding	Bondo-Acetone After Sanding
APC [Control]	3.704	N/A	N/A	N/A	N/A
ABS	42.472	14.862	6.477	3.735	3.9
PETG	30.177	44.488	4.382	5.133	9.191
PETG-CF	47.566	16.508	8.854	11.738	7.021
PLA	25.604	10.433	11.581	5.939	7.673

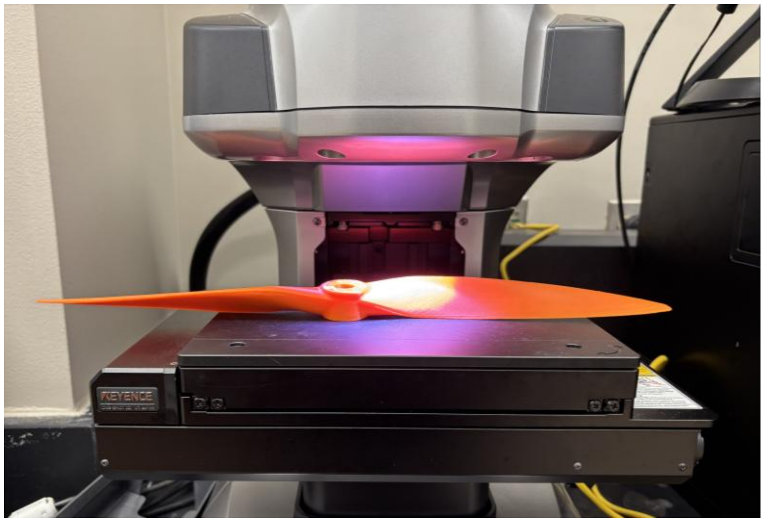

Fig. 5 Keyence VR Machine Operation Setup

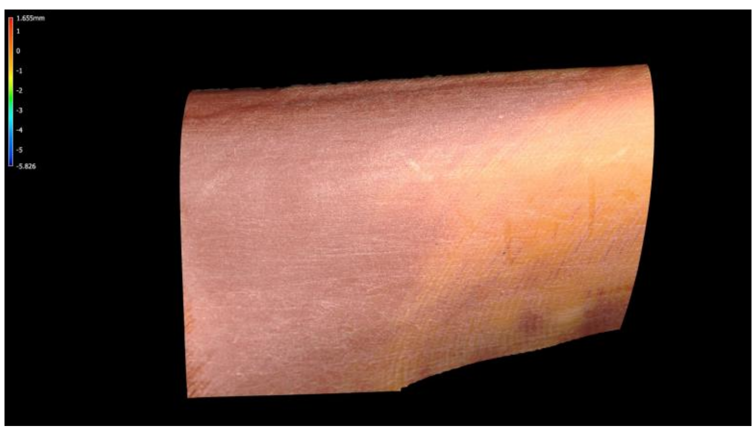
Fig. 6 Surface Roughness Scan from Keyence VR Machine

F. Finishing and Smoothing

To begin the smoothing process, a 2:1 mass ratio of Bondo to acetone was combined and mixed until homogenous. Each propeller used between 6 and 10 grams of Bondo and 3 to 5 grams of acetone, depending on the humidity and weather, as this seemed to affect the evaporation speed of the acetone. This mixture was then applied in three separate thin coats to the propellers with a foam brush. Once completely cured, a progressive sanding procedure was performed to achieve a uniform aerodynamic surface. Sanding began with 110-grit sandpaper to remove excess filler and reduce any prominent surface irregularities, followed then 320-grit, 800-grit, and 1000-grit sandpaper to refine the surface finish. This method allows the Bondo-acetone mixture to fill the surface valleys created by the layer lines that are unavoidable in additive manufacturing, while subsequent sanding reduced the thickened layer ridges down to a common level. The resulting surface profile significantly reduced measurable roughness and more closely approximated that of the commercial baseline propeller from APC.

G. Propeller Modeling and Manufacturing

With the optimal propeller manufacturing techniques fully defined and the XROTOR simulations run, a 3D model of the top 3 propeller geometries was needed. XROTOR outputs a .dat file that contains a table detailing r/R (the non-dimensional radius position), C/R (chord divided by the blade radius), and Beta0deg (blade angle in degrees) at 30 stations along the length of the blade. MATLAB codes (Airfoil_refinery.m & XROTOR_To_CAD.m) [8], Were developed to take the geometry of a given airfoil and the XROTOR output file for a given propeller and output 30 text files containing the geometry of each station along the blade in XYZ coordinates. Two additional files were generated for a set of leading edge and trailing edge points. Using the Insert Curve From XYZ Points function in SolidWorks Section01.tx was imported. A plane was created for Section01 using the imported curve as a reference. Then a sketch was created on the new plane, and Convert Entities was used to convert the curve into a sketch. Section01 was closed with a tangent arc on the trailing edge. This process was repeated for sections 02-30. Both the leading and trailing edge were imported using the Insert Curve From XYZ Points function. They were saved as 3D sketches (See Figure 7).

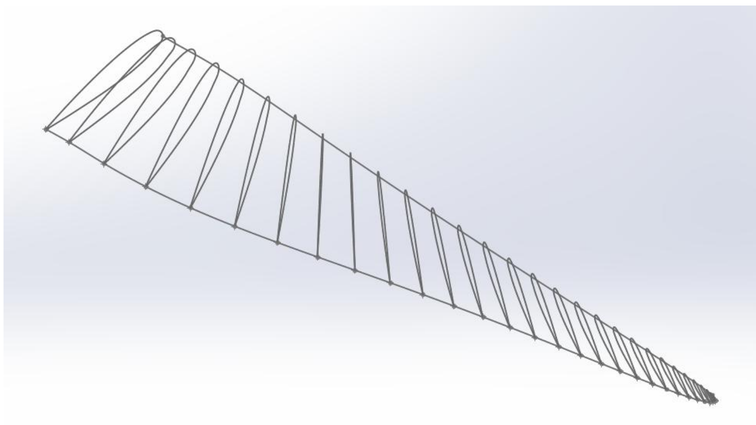

Fig. 7 3117 Prop Blade Skeleton

Lofted Boss/Base used sections 01-30 as sections and the leading and trailing edge curves as guidelines to create a solid blade geometry. To ensure proper fit with the 0.75" hub radius, the blade was extended and cut accordingly. To achieve a pitch of 16 for the propeller, the blades were rotated to an angle of attack of 23 degrees. This is the pitch angle at 75% of the chord for the APC 16x16 propeller. In an assembly, the blade and hub were mated, and the blade was patterned 180 degrees to form a full propeller (Figure 8).

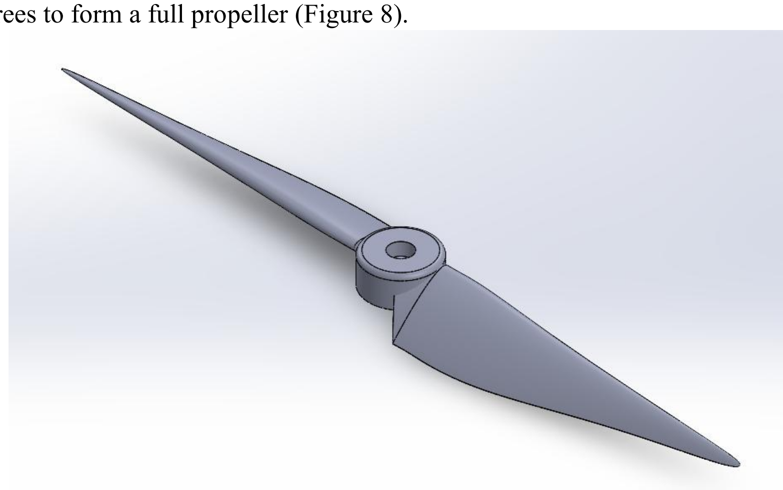

Fig. 8 3117 Blade Propeller SolidWorks CAD

The assembly was saved as a .SDLPRT and then as an .STL file to be used for printing. This process was conducted for the 3117, 4118, and 5213 propeller geometries. All three propellers were printed from ABS and smoothed with acetone-thinned Bondo Glazing and Spot Putty and then sanded. An example is shown in Figure 9.

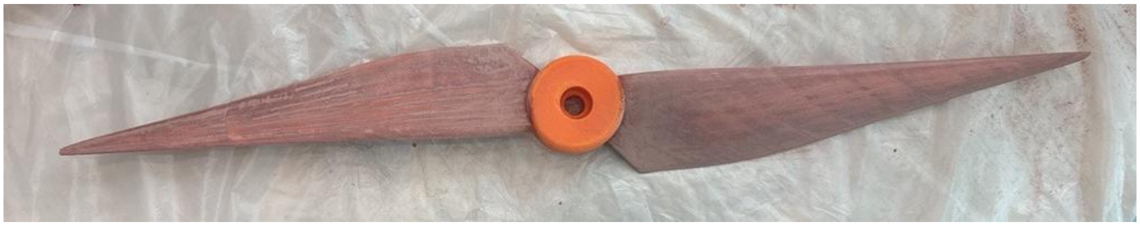

Fig. 9 Propeller Test Article

H. Aerodynamic Performance Testing

With all three propellers manufactured, it was time to test. We tested on the rotor stand (Figure 10) using an ATI F/T Sensor Gamma Load Cell and a custom LabVIEW Virtual Instrument (VI) and data acquisition system, to collect aerodynamic performance data.

Fig. 10 Rotor Test Stand

III. Results & Discussion

A. Data Analysis & Discussion

Using the techniques outlined in the methodology section, three propellers were designed using NACA 3117, 4118, and 5213 airfoils. For each propeller, the following aerodynamic data was collected: thrust (T), torque (Q), coefficient of thrust (C_T), and coefficient of torque (C_Q). This data was collected for each propeller from 1500 to 6000 RPMs for 5 seconds at 500 RPM increments. The performance data from all three propellers and data from APC's website for its 16x16 propellers are co-plotted below in Figure 11.

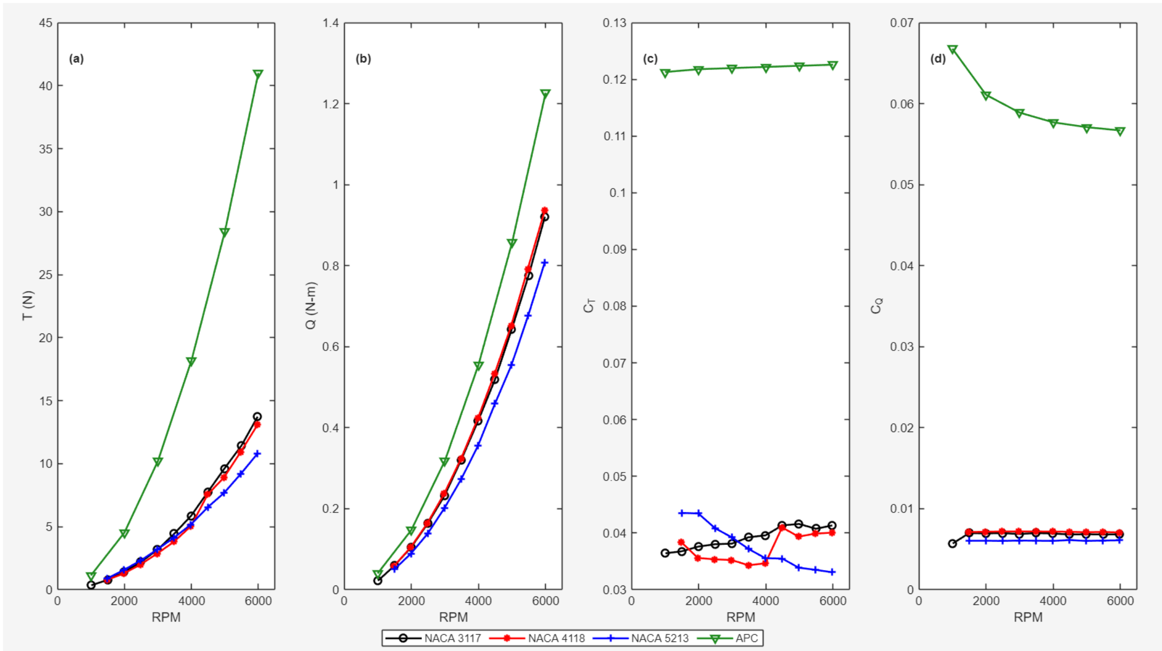

Fig. 11 Coplots of Aerodynamic Data of Manufactured Test Articles to Control APC Propeller

The three test propellers all achieve relatively similar performance numbers, with NACA 5213 achieving the lowest thrust and torque values of the three propellers. When compared to the APC control data, all 3 produce massively less thrust and torque. The APC thrust curve is not only higher in magnitude, but also steeper, while its torque curve is closer to the curves of the 3 test propellers. This is potentially due to the twist in the APC propeller and thus a higher angle of attack in some parts of the blade. Thrust and torque alone were not the only evaluation criteria, however. A propeller's efficiency is calculated as the ratio of the coefficient of thrust multiplied by the advance ratio and then divided by the coefficient of torque. Due to the data collection being conducted on a stationary test stand, the advance ratio for all 3 propellers is zero. The data used from APC's database is for an advance ratio of zero as well. Due to the advance ratio being zero a Static Efficiency Metric (C_T/C_Q) will be used to compare propeller performance. The coefficient of thrust was divided by the coefficient of torque for each RPM and then averaged for each propeller, as shown in Table 2 (all collected aerodynamic data is included in the Appendix).

Table 2 Static Efficiency Metric (C_T/C_Q) Averages

Propeller Type	NACA 5213	NACA 3117	NACA 4118	APC
Average Efficiency Ratio	6.310	5.868	5.227	2.051

This analysis shows that although the APC propeller outperformed the test propellers in raw thrust output, all three test propellers showed far greater efficiency, with the NACA 5213 propeller over tripling the efficiency of the APC propeller. While the lower pitch angle in all three test propellers resulted in lower thrust output, it resulted in lower required torque to spin the propeller. The blades on all three test propellers were the same radius as the APC propeller, but they had a much larger surface area. Of the three test propellers, NACA 5213 was the thinnest and performed the best.

To prove the efficacy of these propellers in practical drone applications, further testing outside the scope of this study is required. Testing propeller performance in a wind tunnel at various air speeds would provide a picture of efficiency at different operational conditions. Extensive flutter testing with a high-speed camera coupled with structural fatigue testing is needed to establish the durability and lifecycle of an additively manufactured propeller. Collecting acoustic data on these propellers is also essential when trying to operationalize a high-lift propeller. There are also far more design variables, such as varying twist angle and multiple airfoils, which could be modified to increase efficiency or improve performance in the above listed tests. Ultimately, the aerodynamic performance data proves the robust nature of our design and manufacturing processes and opens the door to rapid propeller development through iterative design supported by practical testing results.

IV. Conclusion

The goal of this exercise is to compare a commercially available propeller to those derived from a design and additive manufacturing method available to most anyone, without the need for advanced computing or manufacturing hardware. Multiple factors were considered in the design, from propeller size, diameter, airfoil selection, material type, and surface smoothing methods. Ultimately, three propellers were designed with XROTOR using NACA airfoils 3117, 4118, and 5213. These geometries were printed out of ABS, coated with a 2:1 Bondo-acetone mixture, and smoothed with sanding. These three propellers demonstrated almost triple the efficiency of an APC 16x16 propeller. There are still considerations to be made that affect all resulting outcomes, especially regarding aerodynamic flutter and acoustics. This research could be expanded for many use cases by incorporating more factors like varying airfoil shape along propeller blades, vortex generators, winglets, and varying angle of twist during the optimization process. The purpose of this study was to demonstrate that low fidelity aerodynamic modeling techniques coupled with additive manufacturing can produce a viable test article for aerodynamic performance data collection. Overall, the collected performance data indicates that the methodology defined in this paper can produce a propeller that outperforms a commercially available propeller when evaluated on the parameter the design is optimized for. This opens the door to further design and research into the development of high efficiency propellers for use on heavy lift UAVs.

Appendix

Table 3 NACA 5213 Propeller Data

RPM	**Thrust** (N)	**Torque** (N*m)	C_T	C_Q	**Efficiency**
1493	0.889	0.05	0.0435	0.00602	7.225
1990	1.575	0.089	0.0434	0.00603	7.191
2485	2.309	0.138	0.0408	0.00600	6.799
2985	3.199	0.201	0.0392	0.00606	6.468
3487	4.137	0.273	0.0371	0.00603	6.158
3984	5.164	0.355	0.0355	0.00601	5.911
4488	6.543	0.459	0.0354	0.00612	5.793
4978	7.683	0.554	0.0338	0.00600	5.636
5476	9.194	0.676	0.0334	0.00605	5.527
5967	10.778	0.807	0.0330	0.00609	5.427

Table 4 NACA 4118 Propeller Data

RPM	**Thrust** (N)	**Torque** (N*m)	C_T	C_Q	**Efficiency**
1481	0.771	0.058	0.0383	0.00710	5.402
1978	1.275	0.104	0.0355	0.00714	4.982
2478	1.988	0.164	0.0353	0.00717	4.926
2980	2.863	0.237	0.0352	0.00717	4.909
3478	3.799	0.323	0.0343	0.00717	4.779
3985	5.034	0.423	0.0346	0.00716	4.836
4483	7.540	0.534	0.0409	0.00714	5.738
4971	8.901	0.651	0.0393	0.00708	5.556
5466	10.906	0.792	0.0398	0.00712	5.596
5973	13.079	0.937	0.0400	0.00705	5.672

Table 5 NACA 3117 Propeller Data

RPM	**Thrust** (N)	**Torque** (N*m)	C_T	C_Q	**Efficiency**
1496	0.765	0.059	0.0367	0.00697	5.269
1990	1.385	0.104	0.0375	0.00694	5.412
2487	2.186	0.163	0.0380	0.00697	5.450
2989	3.167	0.232	0.0381	0.00686	5.547
3483	4.427	0.32	0.0392	0.00697	5.622
3990	5.86	0.417	0.0395	0.00692	5.711
4487	7.737	0.518	0.0413	0.00680	6.070
4986	9.614	0.642	0.0415	0.00683	6.085
5493	11.427	0.776	0.0407	0.00680	5.984
5977	13.727	0.921	0.0413	0.00682	6.057

Table 6 16x16 APC Propeller Data [3]

RPM	**Thrust** (N)	**Torque** (N*m)	C_T	C_Q	**Efficiency**
1000	1.127	0.04	0.1213	0.0668	1.815
2000	4.525	0.147	0.1218	0.0611	1.993
3000	10.202	0.318	0.1220	0.0589	2.071
4000	18.168	0.555	0.1222	0.0577	2.117
5000	28.433	0.857	0.1224	0.0571	2.143
6000	41.013	1.227	0.1226	0.0567	2.162

Acknowledgments

The group would like to thank Dr. Matthew Priddy, Dr. Shreyas Narsipur, Rob Wolz, Joseph “Drew” Harris, and Sulav Thapa.

References

[1] Aminuddin, A. B., and Salim, W. S. I. W., “Aerodynamic Analysis of Propeller for Heavy Lifting Drone Applications Using Blade Element Momentum Analysis,” *Progress in Aerospace and Aviation Technology*, Vol. 2, No. 2, 2022, pp. 24–32, https://doi.org/10.30880/paat.2022.02.02.004.

[2] Drela, M., “XFOIL: An analysis and design system for low Reynolds ...,” XFOIL: An Analysis and Design System for Low Reynolds Number Airfoils Available: https://web.mit.edu/drela/Public/papers/xfoil_sv.pdf.

[3] Propellers, A., “Performance data,” APC Propellers Available: https://www.apcprop.com/technical-information/performance-data/?v=7516fd43adaa.\

[4] Aeroratech, *Motor Specification Sheet*, May 2025, Aeroratech, https://www.aeroratech.com/wp-content/uploads/2025/05/Motor.pdf

[5] GrabCAD, “GrabCAD Community,” Stratasys Inc., Waltham, MA, accessed Nov. 24, 2025, https://grabcad.com

[6] APC Propellers, "16x16," APC Propellers, Landing Products Inc., Woodland, CA, accessed Feb. 24, 2026, https://www.apcprop.com/product/16x16/.

[7] The MathWorks, Inc., MATLAB® R2025a, Natick, MA, 2025, https://www.mathworks.com/products/matlab.html.

[8] Singleton, D., “Senior-Seminar-Code”. Available: https://github.com/Dalton-S1/Senior-Seminar-Code.